Identifying hidden common causes from bivariate time series: A method using recurrence plots

Yoshito Hirata[*] and Kazuyuki Aihara

Institute of Industrial Science, The University of Tokyo, Tokyo 153-8505, Japan

We propose a method for inferring the existence of hidden common causes from observations of bivariate time series. We detect related time series by excessive simultaneous recurrences in the corresponding recurrence plots. We also use a noncoverage property of a recurrence plot by the other to deny the existence of a directional coupling. We apply the proposed method to real wind data.

PACS number(s): 05.45.Tp, 05.10.−a, 05.45.Vx, 07.05.Kf

I. INTRODUCTION

Since the existence of common causes sometimes leads to wrong conclusions about relations among elements [1,2], distinguishing the influence of hidden common causes from that of directional couplings is an important but unsolved notorious problem. Identifying directional couplings from observed time series is a ubiquitous problem in complex networks and one often encounters the problem of hidden common causes due to unobserved variables. Until now, many methods were proposed for identifying coupling directions from observed time series [3–11]. There are at least 6 major types of methods: methods using mutual prediction [3,4], methods using state space [5], methods using phase modeling [6], methods quantifying information [7–9], methods using partial directed coherence [10], and methods using conditional probabilities of recurrence [11]. However, there is no method so far that can identify the existence of hidden common causes forcing two elements given observations of the forced elements only.

In this paper, we propose a method to identify the existence of hidden common causes using recurrence plots and delay coordinates. When recurrence plots are obtained by appropriate delay coordinates and thresholds, the recurrence plot of the driving force can cover that of the forced system. The advantage of the proposed method is that one can deny directional couplings.

The rest of the paper is organized in the following way. In Sec. II, we introduce background knowledge of recurrence plots and delay coordinates. In Sec. III, we develop the proposed method. In Sec. IV, we present examples. In Sec. V, we conclude this paper.

II. BACKGROUND KNOWLEDGE

First, we introduce background knowledge necessary for understanding the proposed method.

A. Recurrence plots

Recurrence plots [12,13] are two-dimensional plots visualizing time series. Suppose that a time series $x(i)(i=1,2,\ldots,n)$ is given. Using a threshold ϵ_x, we can define a recurrence plot $R_{i,j}^x$ as

$$R_{i,j}^x = \begin{cases} 1 & \text{if } \|x(i)-x(j)\| < \epsilon_x \\ 0 & \text{otherwise.} \end{cases} \qquad (1)$$

When $R_{i,j}^x=1$, a point is plotted at (i,j), otherwise nothing is plotted. The recurrence plot can also be expressed using the Heaviside function Θ as $R_{i,j}^x=\Theta[\epsilon_x-\|x(i)-x(j)\|]$.

In a recurrence plot of Gaussian noise, points spread uniformly and randomly. In a recurrence plot of periodic orbits, points show a periodic pattern, typically long diagonal lines equally spaced. In a recurrence plot of deterministic system such as a logistic map, short diagonal segments appear. Diagonal lines in recurrence plots are typical characteristics of deterministic systems since in a deterministic system, once two points become neighbors, they keep staying close to each other for a while along the time.

One can understand that recurrence plots fundamentally contain almost all information of time series except for the spatial scale since the rough shape of time series can be reproduced from recurrence plots [14,15]. Therefore, from recurrence plots, one can obtain various dynamical invariants such as correlation entropy [16,17] and correlation dimension [16,17]. Moreover, if two time series yield the same recurrence plot, then the corresponding dynamics are equivalent [18].

An extension of recurrence plots to multivariate data is joint recurrence plots [12,19]. Suppose that we have already calculated recurrence plots $R_{i,j}^x$ and $R_{i,j}^y$ for time series x and y. Then their joint recurrence plot $J_{i,j}^{x,y}$ can be defined as an intersection between sets of points plotted for the two recurrence plots. Joint recurrence plots are used for identifying synchronization between two time series, for example [19].

B. Delay coordinates

When obtaining a recurrence plot, we use delay coordinates [20,21] and reconstruct phase space. Let K be a k-dimensional manifold. Let $f:K\to K$ be a map representing a dynamical system $x(t+1)=f[x(t)]$. Denote by $h:K\to R$ its observation function $s(t)=h[x(t)]$. Delay coordinates D with dimension d can be defined as

$$D[x(t)] = \{s(t), s(t-\tau), \ldots, s[t-(d-1)\tau]\}. \qquad (2)$$

When $d\geq 2k+1$, then $D(x)$ and x are one-to-one under mild technical conditions.

*yoshito@sat.t.u-tokyo.ac.jp
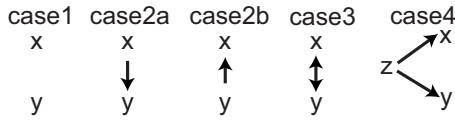
FIG. 1. Elementary relations between two time series x and y.

Stark [22] extended the above theorem for reconstruction of forced systems. Let L be a l-dimensional manifold. Let $f:K \rightarrow K$ be a map of driving force $x(t+1)=f[x(t)]$. Then, we consider a forced system $g:L \times K \rightarrow L$, for which we have $y(t+1)=g[y(t),x(t)]$. In addition, denote an observation function by $h:L \rightarrow R$. We have observations $s(t)=h[y(t)]$. Then, delay coordinates are defined as

$$D[y(t)] = \{s(t),s(t-\tau), \ldots ,s[t-(d-1)\tau]\}. \quad (3)$$

When $d \geq 2(k+l)+1$, then $D(y)$ and (x,y) become one-to-one under mild technical conditions. Sauer [23] used this reconstruction of forced systems to identify driving forces from observations of multiple forced systems.

III. PROPOSED METHOD

To establish algorithm for identifying hidden common causes, we first construct a test for investigating whether two time series are related to each other or not. Then, we deny directional couplings. We use recurrence plots obtained by delay coordinates whose dimension is sufficiently large.

A. Identifying related time series

We classify the relation of two time series into the following 4 cases (Fig. 1): (1) two systems x and y are independent; (2) x (or y) drives y (or x) unidirectionally; (3) x and y are mutually coupled; (4) x and y are driven by a common driving force z.

Let us consider case (1). In this case, delay coordinates $D(x)$ and $D(y)$ are reconstructions of x and y, respectively. Since x and y are independent, $D(x)$ and $D(y)$ are independent. Therefore, the corresponding recurrence plots are also independent.

In case (2a), $D(x)$ corresponds to x and $D(y)$ corresponds to (x,y). Therefore, $D(x)$ and $D(y)$ are not independent. The corresponding recurrence plots are not independent and show excessive simultaneous recurrences. We also call a unidirectional coupling from x to y as case (2a) and a unidirectional coupling from y to x as case (2b).

In case (3), delay coordinates $D(x)$ and $D(y)$ are both reconstructions of (x,y). Therefore, $D(x)$ and $D(y)$ are not independent. The corresponding recurrence plots show excessive simultaneous recurrences.

In case (4), delay coordinates $D(x)$ and $D(y)$ correspond to (x,z) and (y,z), respectively. Therefore, $D(x)$ and $D(y)$, and hence their corresponding recurrence plots, are not independent. The corresponding recurrence plots show excessive simultaneous recurrences. Therefore, by using the above arguments, we can distinguish case (1) from the others.

Let p be the recurrence rate of time series x, namely, the probability that a point is plotted when we choose (i,j) ran-

domly. Similarly, let q be the recurrence rate of time series y. Let u be the joint recurrence rate of x and y, namely, the recurrence rate of joint recurrence plot for x and y. The significance of excessive simultaneous recurrences can be quantified by testing whether a point in the recurrence plot of x is independent of a point of in the recurrence plot of y, namely,

$$u \underset{?}{=} pq. \quad (4)$$

Let $m = \frac{1}{2}(n-1)n$. This m corresponds to the number of independent components in a recurrence plot. When points in recurrence plots of x and y are independent, the joint recurrence plot has the recurrence rate of pq and the number of simultaneous recurrences follows the binomial distribution of size m and probability pq. Since m is usually large, the binomial distribution can be approximated by the normal distribution of mean mpq and variance $mpq(1-pq)$. Let n be the number of simultaneous recurrences. By using the approximation by the normal distribution,

$$z = \frac{n - mpq}{\sqrt{mpq(1-pq)}}, \quad (5)$$

follows the normal distribution of mean 0 and variance 1.

To suppress spatial correlation in a recurrence plot, we subsample data sets by $d\tau$. For the test of relations, we used $p=q=0.05$, namely, we adjusted thresholds for both recurrence plots so that their recurrence rates become $p=q=0.05$. Moreover, we chose the 1% point ($z=2.326$) for judging the significance. We call this test as an independence test.

B. Denying directional couplings

By using recurrence plots obtained by delay coordinates, we can also deny the existence of directional couplings. Suppose that there is a directional coupling from x to y. In this case, $D(y)$ corresponds to (x,y). In short, we write $D(y) \bowtie (x,y)$. In case that there is no directional coupling from y to x [case (2a)], $D(x)$ corresponds to x [$D(x) \bowtie (x)$]. In case that there is also a directional coupling from y to x [case (3)], $D(x)$ corresponds to (x,y) [$D(x) \bowtie (x,y)$]. In either case, if states of two corresponding times are neighbors in $D(y)$, so they are in $D(x)$ as well: if there is no directional coupling from y to x, if two times are in neighbors in $D(y) \bowtie (x,y)$, so they are in $D(x) \bowtie x$; If there is a directional coupling from y to x, then neighbors in $D(x) \bowtie (x,y)$ mean neighbors in $D(y) \bowtie (x,y)$ and vice versa. Therefore, if we choose the thresholds for recurrence plots appropriately, the recurrence plot obtained by $D(x)$ can cover that of $D(y)$. By letting X and Y be points plotted in a recurrence plot of $D(x)$ and $D(y)$, respectively, it holds that $X \supset Y$. Namely, we can choose thresholds so that $X \supset Y$ holds if and only if neighbors in $D(y)$ mean neighbors in $D(x)$. This can be regarded as a rephrase of the continuity for the mapping from $D(y)$ to $D(x)$.

An important point, however, is that when we use this relation for analysis, we have to use the contraposition, which is, if we cannot choose thresholds such that the recurrence plot obtained by $D(x)$ can cover that of $D(y)$, then x does not drive y. Therefore, we can use this inclusive relation for denying directional couplings.

Let use consider the converse, namely, whether or not we can say "if we can choose thresholds so that $X \supset Y$, then x drives y." To investigate this problem, we need to divide it into cases.

First, consider case (2). Considering case (2a) is enough since the similar argument holds for case (2b). Since x drives y in case (2a), based on the above argument, we can say that neighbors in $D(y)$ are also neighbors in $D(x)$. Here $D(x) \bowtie x$ and $D(y) \bowtie (x, y)$. If there is generalized synchronization, then we have a function a such that $y = a(x)$ [24], namely, the driver decides the behavior of the driven system completely. In this case, since $D(y)$ corresponds to $[x, a(x)]$, neighbors in $D(x)$ are also neighbors in $D(y)$. If there is not generalized synchronization, then we do not have a function a such that $y = a(x)$. Then, there are some degrees of freedom left in space y. Therefore, neighbors in $D(x)$ are not necessarily neighbors in $D(y)$.

Second, consider case (3). In this case, both $D(x)$ and $D(y)$ correspond to (x, y), i.e., $D(x) \bowtie (x, y) \bowtie D(y)$. Therefore, times are in neighbors in $D(x)$ if and only if they are neighbors in $D(y)$.

Third, consider case (4). In this case, $D(x)$ corresponds to (x, z) and $D(y)$ corresponds to (y, z), i.e., $D(x) \bowtie (x, z)$ and $D(y) \bowtie (y, z)$. If neither x nor y are generalized synchronized with z, then there are some degrees of freedom in spaces x and y. In this case, therefore, neighbors in $D(x)$ do not mean neighbors in $D(y)$ and vice versa. If x is generalized synchronized with z, and y is not generalized synchronized with z, there is a function b such that $x = b(z)$. Then $D(x)$ corresponds to $[b(z), z]$ and $D(y)$ corresponds to (y, z). Since $D(x)$ only depends on z, neighbors in $D(y)$ mean neighbors in $D(x)$. The similar logic holds when x is not generalized synchronized with z, and y is generalized synchronized with z. If x and y are generalized synchronized with z, there are functions b and c such that $x = b(z)$ and $y = c(z)$. Then since $D(x)$ and $D(y)$ correspond to $[b(z), z]$ and $[c(z), z]$ respectively, times are in neighbors in $D(x)$ if and only if they are in neighbors in $D(y)$.

We summarize the above relations. If neighbors in $D(x)$ and those in $D(y)$ are equivalent, then the case should be case (2) with generalized synchronization $y = a(x)$, case (3), or case (4) with generalized synchronization $x = b(z)$ and $y = c(z)$. If neighbors in $D(y)$ mean neighbors in $D(x)$ but the opposite is not true, then the case should be case (2) without generalized synchronization or case (4) with generalized synchronization $x = b(z)$ or $y = c(z)$. If neighbors in $D(y)$ do not mean neighbors in $D(x)$ and vice versa, then the case should be case (4) without generalized synchronization. In the above relations, the condition that neighbors in $D(y)$ mean neighbors in $D(x)$ can be rephrased as the condition that there is a set of thresholds for recurrence plots such that $X \supset Y$ holds.

When actually testing the inclusive relation, we may fix the threshold of x and gradually decrease that of y, and stop at the point where the inclusive relation holds. If the number of points plotted for $D(y)$ is not significantly large in terms of Eq. (5), then we consider that the directional coupling from x to y is not likely to exist.

Alternatively, we can compare the recurrence plot of x obtained using a fixed ϵ_x with that of y obtained using the best threshold. We can find the best threshold of y by finding
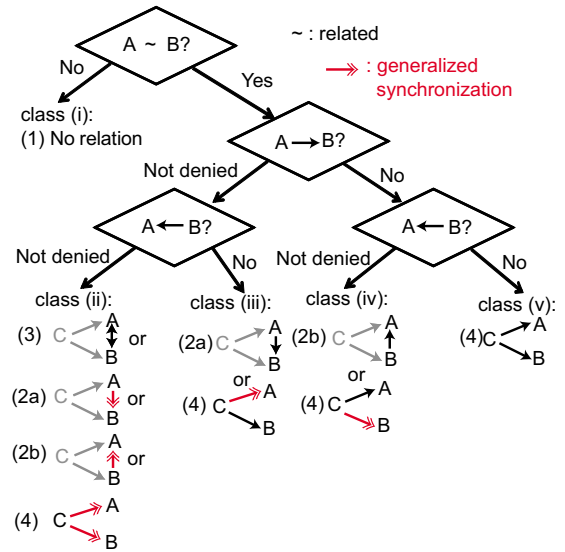
FIG. 2. (Color online) Algorithm for identifying coupling types. Directional couplings are shown in single arrows and generalized synchronization is shown in double arrows. Elements which may not exist are shown in gray.

the minimum significant recurrence rate q of y, which satisfies Eq. (5) with $\mathcal{n} = mq$:

$$z_r = \frac{mq - mpq}{\sqrt{mpq(1 - pq)}}, \quad (6)$$

where p is the recurrence rate for the recurrence plot of x and z_r is the $100r$ percentile point of the normal distribution from the above. Throughout the paper, we set $r = 0.01$. Therefore, in this paper, each test for denying directional coupling has the significance level of 0.01. We also choose $p = 0.5$ since if p is small, then q become too small so that the recurrence plot of y contains only few points. By solving Eq. (6) in terms of q, we can obtain

$$q = \frac{z_r^2 mp}{m^2(1 - p)^2 + z_r^2 mp^2}. \quad (7)$$

We call this test as a test for a directional coupling.

C. Summary of algorithm

We summarize the algorithm for identification of coupling types in Fig. 2. At the beginning, we test whether two time series are related or not. If there is no relation, then they are likely to be independent [class (i)]. If there is likely to be some relations, then we test directional couplings. First, we test a directional coupling from one time series to the other. Second, we test the opposite directional coupling. If directional couplings for both directions are denied, the influence of the common third element is likely to exist [class (v)]. If only one directional coupling is denied, then we have either the opposite directional coupling or influence of the common third element [class (iii) or class (iv)]. If both directional couplings are not denied, then we cannot conclude anything about couplings and all 4 possibilities remain [class (ii)]. In
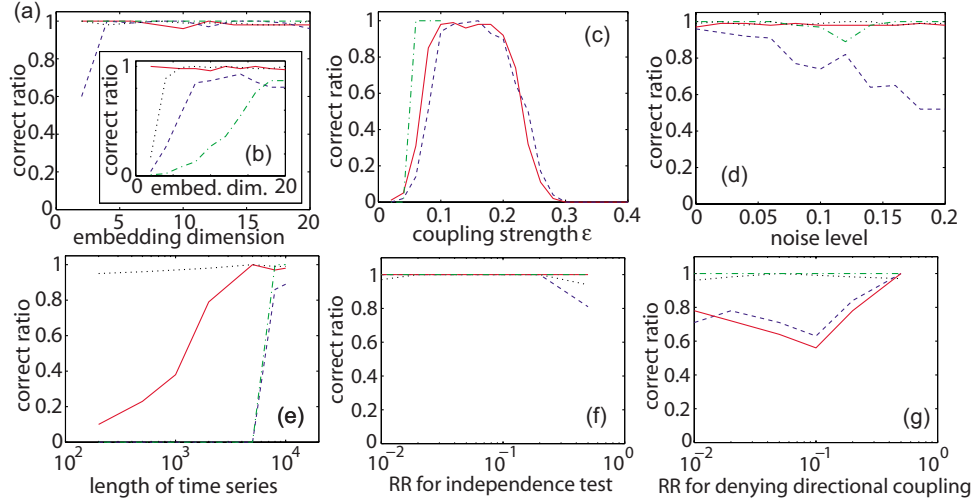
FIG. 3. (Color online) Effects of (a) (b) embedding dimension, (c) coupling strength, (d) noise level, (e) length of time series, (f) recurrence rates during the independence test, and (g) recurrence rate during denying directional couplings. For (a), we used clean data. For (b), we added 10% observational noise. For each graph, the black dotted line corresponds to case (1), the blue dashed line corresponds to case (2a), the green dash-dotted line corresponds to case (3), and the red solid line corresponds to case (4). For (f) and (g), we used the 5-dimensional embedding space.

class (iii) and class (iv), the main couplings are direct couplings between A and B. As far as we tested, the influence of the common third C may appear when generalized synchronization exists between two systems. The similar argument applies to class (ii).

We also need to remark a point here. Since what we can do is to deny the existence of directional coupling, the common third element might coexist in cases (2a), (2b), and (3) of class (ii), case (2a) of class (iii), and case (2b) of class (iv), which are shown in gray in Fig. 2. We have another point to remark. Directional couplings detected by the proposed method may be indirect ones going through other elements. Therefore, when interpreting the results, we must take into account this point.

IV. EXAMPLES

A. Example 1: Elementary relations

First, we tested examples of elementary relations. The model first tested was where there are two independent elements [case (1)],

$$x_{t+1} = 3.81x_t(1 - x_t), \tag{8}$$

$$y_{t+1} = 3.82y_t(1 - y_t). \tag{9}$$

The second tested was the model where two elements were coupled unidirectionally [case (2)],

$$x_{t+1} = 3.81x_t(1 - x_t), \tag{10}$$

$$y_{t+1} = (1 - \epsilon)3.82y_t(1 - y_t) + \epsilon 3.81x_t(1 - x_t). \tag{11}$$

The third tested model was the model where two maps were coupled bidirectionally [case (3)],

$$x_{t+1} = (1 - \epsilon)3.81x_t(1 - x_t) + \epsilon 3.82y_t(1 - y_t), \tag{12}$$

$$y_{t+1} = (1 - \epsilon)3.82y_t(1 - y_t) + \epsilon 3.81x_t(1 - x_t). \tag{13}$$

The fourth tested model was the model where two maps have the influence from the common third element [case (4)],

$$z_{t+1} = 3.8z_t(1 - z_t), \tag{14}$$

$$x_{t+1} = (1 - \epsilon)3.81x_t(1 - x_t) + \epsilon 3.8z_t(1 - z_t), \tag{15}$$

$$y_{t+1} = (1 - \epsilon)3.82y_t(1 - y_t) + \epsilon 3.8z_t(1 - z_t). \tag{16}$$

In each model, we generated 100 time series of the length 10 000 using different initial conditions. We set $\epsilon = 0.1$ if not mentioned.

We first investigated the effects of embedding dimension [Figs. 3(a) and 3(b)]. The proposed method is effective when the embedding dimension is sufficiently large. In addition, the larger embedding space is, the more immune to observational noise [Fig. 3(b)]. Therefore, in the rest of the paper, we set $d = 20$ if not mentioned. How to choose the embedding dimension optimally is a topic of future research.

The results depend on the coupling strength of systems [Fig. 3(c)]. If the coupling strength is too weak, the proposed method cannot detect the couplings. If the coupling strength is too strong, then elements of systems get synchronized and the relation will be classified as class (ii).

The results got worse when the level of observational noise increased [Fig. 3(d)]. The proposed method seems to give meaningful results when the noise level is 16% or less. In case of dynamical noise, the proposed method is not supported by the embedding theorem.

We also investigated the influence of length of time series [Fig. 3(e)]. If the length of time series is nearly or over 8000, the methods worked correctly.
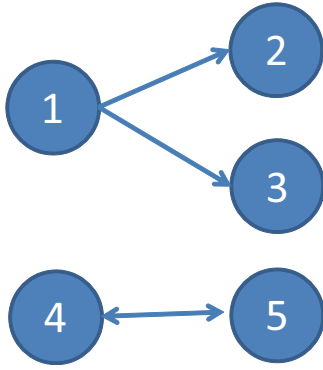
FIG. 4. (Color online) Inferred network from coupled Rössler systems. We assumed that generalized synchronization does not exist.

In addition, we investigate the effects of recurrence rates for the independence test [see Fig. 3(f)]. If the recurrence rates p and q are between 0.02 and 0.2, then classification was appropriate for all models.

Moreover, we looked into the effects of the recurrence rate p for denying directional coupling [see Fig. 3(g)]. When the recurrence rate is 0.5, the tested time series were correctly classified the best. As we discussed previously, if p is too small, then q becomes also too small and the recurrence plot for the "supposed" driven system only contain few points. Therefore, choosing $p=0.5$ seems the best choice for denying directional coupling.

Since each test has the significance level of 1% and there are 3 tests for each data, we expect about 3% for the false classification. For this viewpoint, our test is reasonable since the correct ratio for classification was above 0.97 when the recurrence rates p and q were between 0.02 and 0.2 in Fig. 3(f).

In case (1), we also tested the case where the parameters of two systems were the same,

$$x_{t+1} = 3.81x_t(1 - x_t), \tag{17}$$

$$y_{t+1} = 3.81y_t(1 - y_t). \tag{18}$$

Then, we confirmed that the relation was correctly classified.

B. Example 2: Coupled Rössler systems

We also tested an example of five coupled Rössler systems,

$$\dot{x}_1 = -1.05y_1 - z_1,$$

$$\dot{y}_1 = 1.05x_1 + 0.15y_1,$$

$$\dot{z}_1 = 0.2 + z_1(x_1 - 10), \tag{19}$$

$$\dot{x}_2 = -1.03y_2 - z_2 + \epsilon(x_1 - x_2),$$

$$\dot{y}_2 = 1.03x_2 + 0.15y_2,$$

$$\dot{z}_2 = 0.2 + z_2(x_2 - 10), \tag{20}$$
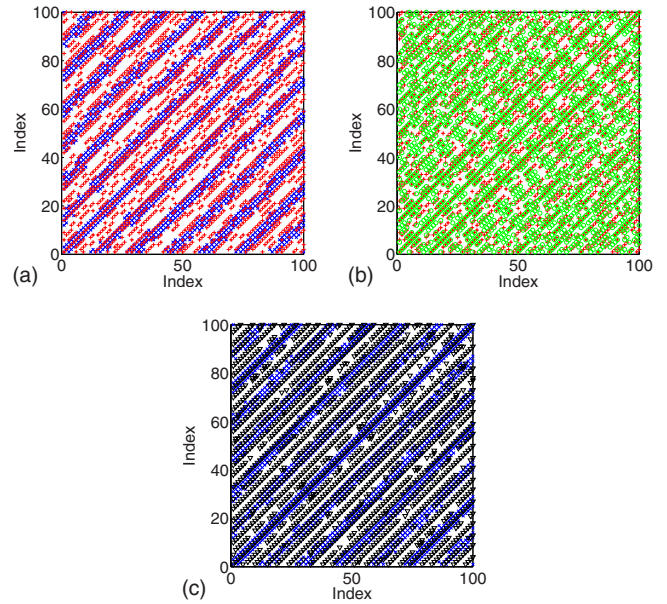
FIG. 5. (Color online) Comparisons of recurrence plots of (a) x_1 (blue ×) and x_2 (red +), (b) x_2(red +), and x_3 (green ○), and (c) x_1 (blue ×) and x_4 (black ▽). Parts of recurrence plots are shown to emphasize the details. Recurrence plots of x_1 and x_2 and those of x_2 and x_3 overlapped significantly (p-value <0.001), respectively, while the overlaps between recurrence plots of x_1 and x_4 are not significant (p-value >0.05).

$$\dot{x}_3 = -1.01y_3 - z_3 + \epsilon(x_1 - x_3),$$

$$\dot{y}_3 = 1.01x_3 + 0.15y_3,$$

$$\dot{z}_3 = 0.2 + z_3(x_3 - 10), \tag{21}$$

$$\dot{x}_4 = -0.99y_4 - z_4 + \epsilon(x_5 - x_4),$$

$$\dot{y}_4 = 0.99x_4 + 0.15y_4,$$

$$\dot{z}_4 = 0.2 + z_4(x_4 - 10), \tag{22}$$

$$\dot{x}_5 = -0.97y_5 - z_5 + \epsilon(x_4 - x_5),$$

$$\dot{y}_5 = 0.97x_5 + 0.15y_5,$$

$$\dot{z}_5 = 0.2 + z_5(x_5 - 10). \tag{23}$$

Here, three subsystems were coupled as case (4) and two other subsystems were coupled as case (3). We set $\epsilon=0.05$. We generated a time series of length 10 000, sampled x_i every 1 unit time.

The inferred network is shown in Fig. 4. During the inference, we compared recurrence plots as shown in Figs. 5 and 6.

C. Example 3: Actual winds

Finally, we applied the proposed method to data sets of winds observed in Hokkaido, the northern island in Japan.
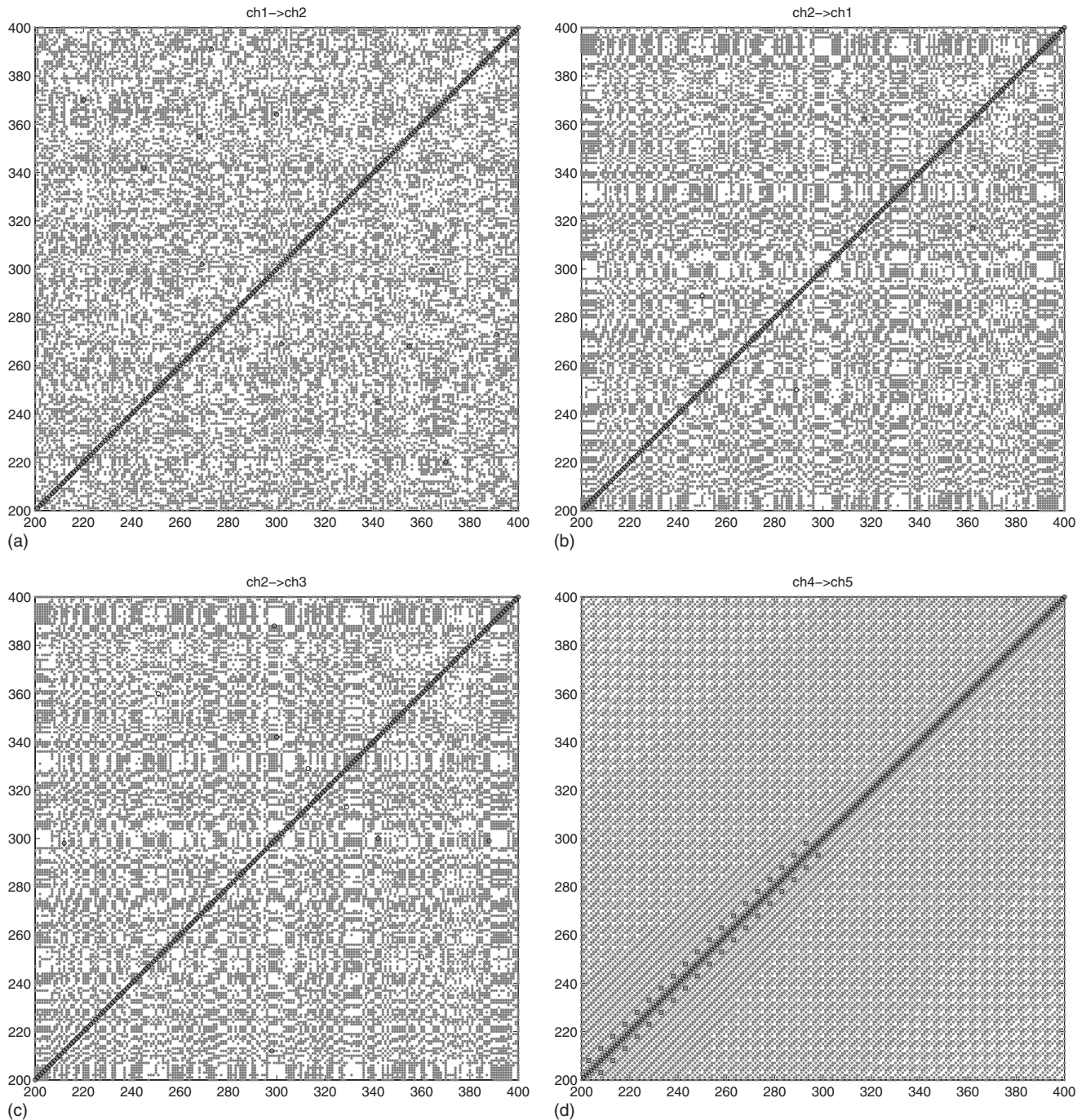
FIG. 6. Tests for directional couplings in coupled Rössler systems. (a) $x_1 \rightarrow x_2$, (b) $x_2 \rightarrow x_1$, (c) $x_2 \rightarrow x_3$, and (d) $x_4 \rightarrow x_5$. Recurrence plots for candidates of driving forces are shown in gray dots and those for candidates of forced systems are shown in black circles. Parts of recurrence plots are shown to emphasize the details.

We used the measurements in July and August 2003. The wind speed and the wind direction were observed every 10 min in Sapporo $(43°04'N, 141°20'E)$ and Hakodate $(41°49'N, 140°45'E)$. The data sets contains 8928 points. By taking the projections, we converted the data sets into those of east and north winds. The data sets were shown in Fig. 7(a). The correlation coefficients between the east and the north winds were -0.79 and -0.32 in Sapporo and Hakodate, respectively. The correlation coefficients between Sapporo and Hakodate were 0.50 and 0.07 in the east and

north winds, respectively. For this data set, we used the embedding dimension between 11 and 20 and chose the most frequently observed class as a selected class. Between the east and the north winds of Sapporo, the inferred relation is class (ii) [Fig. 7(b)], and therefore, it is likely that the bidirectional couplings exist or these winds are synchronized. Between the east and the north winds of Hakodate, the inferred relation is class (iii). Therefore, the unidirectional coupling from the east wind to the north wind may exist. This result is reasonable since the east and north winds at the

V. CONCLUSIONS

In sum, we have proposed a method that identifies related time series and denies the existence of directional couplings by using recurrence plots obtained by delay coordinates. Thus, the proposed method can imply the existence of hidden common causes. We believe that the proposed method helps to give more accurate insights into topological structures of complex networks based on observed time series.

FIG. 7. (a) Observed wind data. The east and north winds in Sapporo are shown in gray and black, respectively. (b) The recurrence plots of east wind in Sapporo (gray dots) cover those of north wind in Sapporo (black circles). Part of recurrence plots is shown here to emphasize the details.

same points can be strongly coupled. Between the winds of Sapporo and Hakodate, the inferred relation is class (v), and thus the existence of hidden common causes was inferred. Candidates of hidden common causes are clouds, high and low pressures, and the sun. We can take into account delays by comparing $R_{i,j}^x$ and $R_{i+k,j+k}^y$. This is a topic of future research.

[1] K. Zadnik, L. A. Jones, B. C. Irvin, R. N. Kleinstein, R. E. Manny, J. A. Shin, and D. O. Mutti, Nature (London) **404**, 143 (2000).

[2] J. Gwiazda, E. Ong, R. Held, and F. Thorn, Nature (London) **404**, 144 (2000).

[3] S. J. Schiff, P. So, T. Chang, R. E. Burke, and T. Sauer, Phys. Rev. E **54**, 6708 (1996).

[4] Y. Chen, G. Rangarajan, J. Feng, and M. Ding, Phys. Lett. A **324**, 26 (2004).

[5] J. Arnhold, K. Kehnertz, P. Grassberger, and C. E. Elger, Physica D **134**, 419 (1999).

[6] M. G. Rosenblum and A. S. Pikovsky, Phys. Rev. E **64**, 045202(R) (2001).

[7] T. Schreiber, Phys. Rev. Lett. **85**, 461 (2000).

[8] M. Palus, V. Komarek, Z. Hrncir, and K. Sterbova, Phys. Rev. E **63**, 046211 (2001).

[9] M. Palus and M. Vejmelka, Phys. Rev. E **75**, 056211 (2007).

[10] M. Winterhalder, B. Schelter, and J. Timmer, Int. J. Bifurcation Chaos Appl. Sci. Eng. **17**, 3735 (2007).

[11] M. C. Romano, M. Thiel, J. Kurths, and C. Grebogi, Phys. Rev. E **76**, 036211 (2007).

[12] N. Marwan, M. C. Romano, M. Thiel, and J. Kurths, Phys. Rep. **438**, 237 (2007).

[13] C. L. Webber, Jr. and J. P. Zbilut, Int. J. Bifurcation Chaos Appl. Sci. Eng. **17**, 3467 (2007).

[14] M. Thiel, M. C. Romano, and J. Kurths, Phys. Lett. A **330**, 343 (2004).

[15] Y. Hirata, S. Horai, and K. Aihara, Eur. Phys. J. Spec. Top. **164**, 13 (2008).

[16] P. Faure and H. Korn, Physica D **122**, 265 (1998).

[17] M. Thiel, M. C. Romano, P. L. Read, and J. Kurths, Chaos **14**, 234 (2004).

[18] G. Robinson and M. Thiel, Chaos **19**, 023104 (2009).

[19] M. C. Romano, M. Thiel, J. Kurths, and W. von Bloh, Phys. Lett. A **330**, 214 (2004).

[20] F. Takens, in *Dynamical Systems and Turbulence*, Lecture Notes in Mathematics Vol. 898, edited by D. A. Rand and L. S. Young (Springer, Berlin, 1981), p. 366.

[21] T. Sauer, J. A. Yorke, and M. Casdagli, J. Stat. Phys. **65**, 579 (1991).

[22] J. Stark, J. Nonlinear Sci. **9**, 255 (1999).

[23] T. D. Sauer, Phys. Rev. Lett. **93**, 198701 (2004).

[24] N. F. Rulkov, M. M. Sushchik, L. S. Tsimring, and H. D. I. Abarbanel, Phys. Rev. E **51**, 980 (1995).